Advances in Bioresearch
Adv. Biores., Vol 16 (3) May 2025: 207-220

Print ISSN 0976-4585; Online ISSN 2277-1573
Journal's URL:http://www.soeagra.com/abr.html
CODEN: ABRDC3
DOI: 10.15515/abr.0976-4585.16.3.207220

Advances in Bioresearch

ORIGINAL ARTICLE

An *In Silico* Drug Discovery Approach Targeting RhoJ: Homology Modelling, Computational Screening and Molecular Docking for Novel Therapeutic Inhibitors

N. Sravanthi, U. S. H. Raghavendra Prasad, N. Ravi, *M. Kavitha
Department of Chemistry, University College of Science, Osmania University, Hyderabad 500007, Telangana, India
*Corresponding author's email: kavithamannem@gmail.com; kavithamannem@osmania.ac.in

ABSTRACT
RhoJ, a member of the Cdc42 subfamily of Rho GTPases, is involved in cytoskeletal dynamics, angiogenesis, and vascular remodeling. Dysregulation or mutation of RhoJ has been linked to various cancers, including breast, bladder, gastric, and brain tumors. These alterations can enhance signaling through effectors like PAK1 and VEGFR2, promoting EMT, tumor angiogenesis, and therapy resistance. Mutant RhoJ may remain in an active GTP-bound state or disrupt normal regulation, fostering a pro-invasive tumor phenotype. These features position RhoJ as both a biomarker of tumor aggressiveness and a potential therapeutic target, although further research is needed to explore its mutation-specific roles and drug ability. In this way advanced computational algorithms are employed to selectively target RhoJ protein and identify prospective inhibitory molecules.
Keywords: *GTPase, Cytoskeletal dynamics, angiogenesis, VEFGR2, EMT*

Received 18.03.2025 Revised 16.05.2025 Accepted 28.05.2025

How to cite this article:
N. Sravanthi, U. S. H. Raghavendra Prasad, N. Ravi, M. Kavitha. An *In Silico* Drug Discovery Approach Targeting RhoJ: Homology Modelling, Computational Screening and Molecular Docking for Novel Therapeutic Inhibitors. Adv. Biores., Vol 16 (3) May 2025: 207-220.

INTRODUCTION

Cancer is a complex group of diseases characterized by uncontrolled cell division and the potential to invade or spread to surrounding tissues and distant organs. It arises from genetic and epigenetic alterations that disrupt the normal regulatory mechanisms of cell growth, apoptosis, and differentiation. These changes often result in the activation of oncogenes, inactivation of tumour suppressor genes, and dysregulation of cellular signalling pathways. Despite advances in early detection and treatment, cancer remains a leading cause of mortality worldwide, prompting continued efforts to identify novel therapeutic targets and develop more effective, personalized treatment strategies.

Rho GTPases [1], a subfamily of the Ras superfamily are critically involved in the regulation of cancer initiation and progression. These molecular switches modulate key cellular functions such as proliferation, motility, invasion, and metastatic spread. Aberrant expression or activity of Rho GTPases has been widely reported across various cancer types. Although certain members may exert tumor-suppressive effects depending on cellular context, many Rho GTPases contribute to oncogenic processes and are associated with more aggressive tumor phenotypes [1-10].

The role of RhoJ protein in Cancer

RhoJ is a small GTPase protein belonging to the Rho family, mainly known for its regulatory function in endothelial cell behavior, angiogenesis, and cytoskeletal dynamics. While RhoJ plays a normal role in maintaining blood vessel stability and guiding cell movement, it becomes significantly involved in cancer progression [11] when its expression or activity is altered. In cancer, RhoJ becomes overexpressed or abnormally activated in tumor cells or tumor-associated endothelial cells. This contributes to several cancer-promoting mechanisms including tumor angiogenesis, epithelial-mesenchymal transition (EMT)

[8], cell survival [12], and Cytoskeletal remodeling [13] and Chemo resistance [14] as depicted in the figure 1.

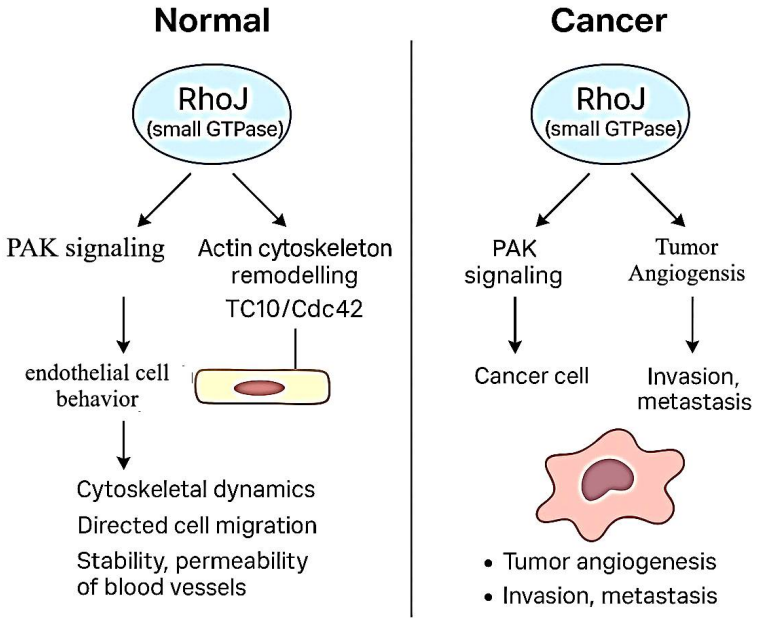

Figure 1: Biochemical Cascade of RhoJ protein

MATERIAL AND METHODS

In recent years, computational methods in chemistry have gained prominence as a means to overcome the limitations of traditional drug discovery processes. Currently, a fully resolved three-dimensional (3D) structure of the RhoJ protein has not been achieved through either experimental techniques or computational modeling. As a result, this chapter centers on the development and validation of a 3D model of RhoJ using computer-based approaches. The RhoJ amino acid sequence, formatted in FASTA, was retrieved from the UniProt database [15]. To identify suitable templates for modeling, proteins with comparable secondary structures, domain architectures, and folding characteristics were selected using tools such as Jpred4 and PHYRE2 [16,17]. The structural similarity between RhoJ and these templates was evaluated using the E-value, a statistical measure that quantifies sequence-to-structure alignment.

Protein sequence alignment and 3D model construction

The target protein's amino acid sequence was aligned with those of template proteins using CLUSTALW [18]. A three-dimensional model of the RhoJ protein was subsequently generated with MODELLER [19], which applies the CHARRMM22 force field during structure prediction. Among the generated models, the one with the lowest objective function score was selected for further refinement and optimization analyses.

Energy minimization and validation

To enhance the accuracy of the constructed 3D protein model, loop regions were refined and energy minimization was performed using the imperf module from the Schrodinger software suite, applying a 0.3 Å cutoff. The process made use of the OPLS 2004 (Optimized Potential for Liquid Simultaneous) force field to maintain the integrity of the protein's native carbon backbone. During minimization, the backbone atoms were kept stationary while allowing side chains to reposition, enabling the structure to achieve a stable, low-energy state without modifying the coordinates of the ca atoms [20].

To improve the stability of the model, molecular dynamics simulations were carried out using the Protein Preparation Wizard available in the Schrodinger Suite. The OPLS-AA (all-atom) force field was employed during this process to refine and optimize the three-dimensional structure [20].

The reliability and accuracy of the homology model were evaluated using tools such as PROCHECK [21], ProSA [22], and VERIFY_3D [23]. To determine how closely the model resembled the template, a root mean square deviation (RMSD) analysis was performed between the target protein, RhoJ, and its template structure. The most stable conformation identified through this analysis was chosen for detailed investigation, focusing on its secondary structural components and possible active site locations.

Active site identification by computational approach

Identifying a protein's active site with precision is essential for understanding its specific biological function and is a key step in structure-based drug design. Computational methods are commonly applied to predict likely ligand -binding sites within the protein's 3D structure. Programs like CASTp and the SiteMap tool in the Schrodinger suite are frequently used to locate hydrophobic pockets and structurally suitable regions for ligand interaction [24, 25].

Virtual Screening and Molecular Docking

To enable virtual screening and molecular docking studies, a receptor grid was constructed at the anticipated binding site of the RhoJ protein using the Glide module from the Schrodinger software suite. Ligand structure were sourced from reputable structural databases and processed using LigPrep [26], which refines their stereochemistry, ionization states, and ring conformations for improved docking accuracy. The virtual screening process was carried out in a stepwise manner employing Glide's HTVS (High Throughput Virtual Screening), SP (Standard Precision), and XP (Extra Precision) protocols [27, 28]. Following docking, ligands were evaluated and ranked according to their Glide Scores, indicative of their predicated binding affinity.

ADMET Properties

Thorough assessment of Absorption, Distribution, Metabolism, Excretion, and Toxicity (ADMET) characteristics plays a vital role in the early stages of drug discovery, as these factors significantly impact the success of a clinical trials and the potential marketability of drug candidates [29,30]. Ligands showing strong binding affinity to RhoJ, identified through virtual screening and docking, were evaluated for their ADME properties using the QuikProp tool available in the Schrodinger suite. Additionally, the Pro Tox 3.0 online platform was utilized to analyze toxicity and ease of synthesis [31]. Compounds with favorable ADME profiles and low predicted toxicity were prioritized as potential therapeutic agents for treating cancer.

RESULTS AND DISCUSSION

Computational modelling-based three-dimensional structural analysis of the RhoJ protein

Retrieval of amino acid sequence data followed by the identification of a suitable structural template for modelling

The UniProt server serves as a pivotal platform in bioinformatics, offering a well-curated and comprehensive database of protein sequences and annotations that underpins diverse biological research areas [15]. Integrating data from Swiss-Prot, TrEMBL, and PIR, UniProt provides extensive information on protein sequences, functional annotations, structural characteristics, and taxonomy its intuitive interface facilitates efficient protein searches through query-based tools, enabling users to retrieve and download FASTA-formatted sequences essential for advanced bioinformatics analyses. In this research, the UniProt server was utilized to extract sequences corresponding to RhoJ protein, which were subsequently examined to obtain functional annotations and structural insights [1]. These sequences played a crucial role in identifying conserved motifs and active sites critical for homology modeling studies. By leveraging accession numbers or sequence-specific queries, UniProt ensured reliable and reproducible results, forming an integral part of the computational workflow.

Template selection

The Basic Local Alignment Search Tool (BLAST) server was utilized to identify an appropriate structural template for RhoJ protein (Table 1), a key protein in Rho GTPases that regulate cytoskeleton dynamics, cell morphology and polarity, cell motility, vesicle trafficking, cell cycle progression, cell survival, cell growth, and differentiation and new gene expression [32]. The protein's FASTA sequence was submitted to the Protein Data Bank (PDB) via the BLASTP algorithm [33]. The selection process prioritized template with high sequence identity, low E-value (<0.001), and extensive query coverage to ensure accurate and reliable structural modeling. Among the results, a template 2ATX_A showing 83.62 % sequence homology with RhoJ Protein.

This template formed the basis for subsequent 3D modeling and structural evaluation, demonstrating the BLAST server's effectiveness in facilitating homology-based protein structure predictions.

To determine the three-dimensional (3D) structure of the target protein, its amino acid sequence in FASTA format was uploaded to the Phyre2 web server (Kelley et al., 2015) [4]. The sequence underwent analysis using a Hidden Markov Model (HMM)-based alignment, where it was compared against structural template available in the Protein Data Bank (PDB). The most suitable template was selected based on sequence identity, alignment coverage, and confidence score. Following template selection, homology modeling was conducted to construct a predicted 3D structure. The constructed 3D model was

further optimized using structural validation tools ProSA and Verify3D. The validated structure plays a crucial role in protein – ligand docking, functional analysis, and drug discovery research.

Table 1: Template selection of RhoJ Protein

S.NO	Template Search Tool	Identified Template	% Identity	E – value / Confidence score
1	PSI – BLAST	2ATX_A	83.62	7 × e-107
2	Jpred4	2ATX_A	82.00	9 × e-98
3	PHYRE2	2ATX_A	81.00	99.8%

c) Sequence –based alignment and structural verification of a computationally modeled RhoJ protein

The RhoJ protein sequence was precisely aligned with homologous sequences from evolutionarily conserved template proteins, establishing a robust basis for reliable three-dimensional structure prediction. Using the RhoJ FASTA sequence and the selected template structure 2ATX_A along with their corresponding atomic coordinates (as shown in Figure 2) - MODELLER [34] was employed to generate a set of 50 structural models. Among these, the model exhibiting the lowest objective function score was chosen for subsequent refinement and structural optimization procedures.

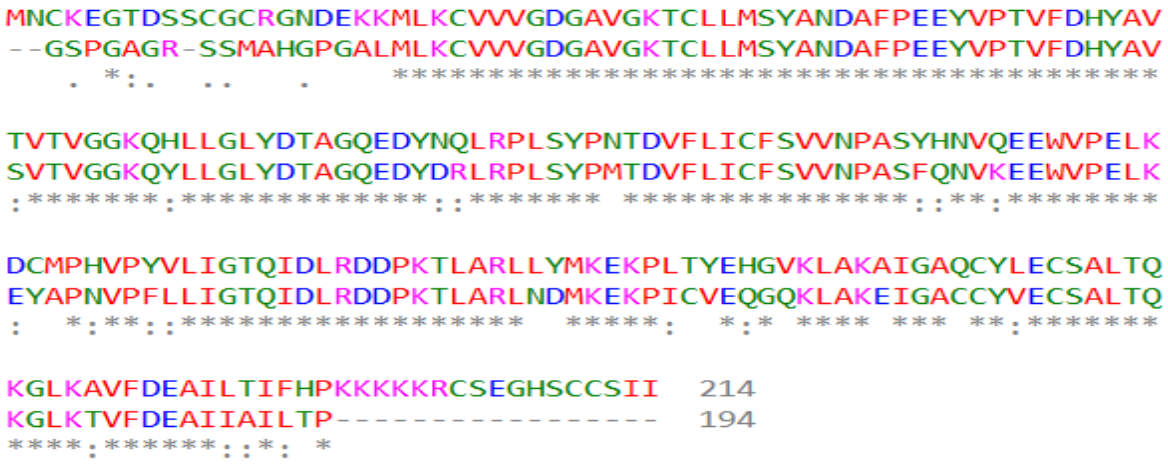

Figure 2: Comparative alignment of the RhoJ protein with the structural template 2ATX_A

Figure 2 Presents the sequence alignment between the target RhoJ protein and its structural template, designated as 2ATX_A. The alignment was performed using the CLUSTALW algorithm and visualized with Discover Studio Visualizer version 24.1.0. The results indicate a sequence identity of 83.62% between RhoJ and the template 2ATX_A. In the alignment visualization, conserved amino acid residues are depicted in red color, residues with strong similarity and shown green color, and those with weak similarity appear in blue. This color-coded scheme effectively highlights the evolutionary conservation patterns across the aligned sequences.

The constructed three – dimensional model underwent further refinement and assessment using structural validation tools, including ProSA and Verify 3D. The validated model serves as a reliable framework for protein-ligand docking analysis, functional characterization, and potential applications in structure-based drug discovery.

Computational validation of *In silico* generated model (Model Validation)

The stereochemical integrity of the RhoJ protein model was evaluated using the Ramachandran plot (3.2). The analysis indicated that 94.1% of the residues are located within energetically favorable regions, reflecting high structural quality. To assess the compatibility of individual amino acids within the three-dimensional environment, the VERIFY_3D tool was employed. This approach evaluates the correspondence between each residue's position in the primary sequence (1D) and its spatial context in the 3D model. The results showed that 86.91% of the 214 amino acids in the RhoJ structure achieved a 3D-1D score greater than 0.2, which falls within the acceptable range.

Additionally, the overall structural quality of the RhoJ model was examined using the ProSA (Protein structural analysis) web server (Figure 3 and 4). ProSA compares the model against known protein structure of similar length in the Protein Data Bank (PDB), evaluating both global and local model reliability.

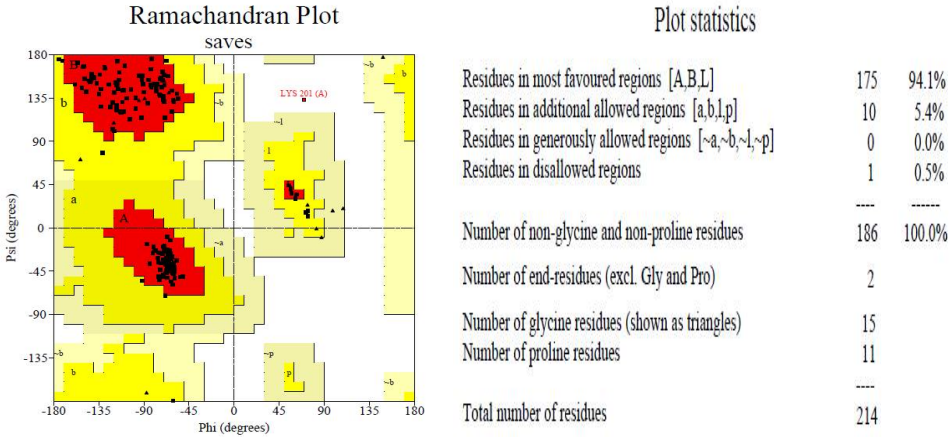

Figure 3: Assessment of stereochemical quality of the RhoJ protein structure using Ramachandran contour diagram

As shown in Figure 3, the Ramachandran plot for the RhoJ protein reveals that 94.1% of its residues are located within energetically favorable regions [35-37]. Protein models in which over 90% of residues fall within these preferred regions are generally regarded as stereochemically stable and of high structural quality.

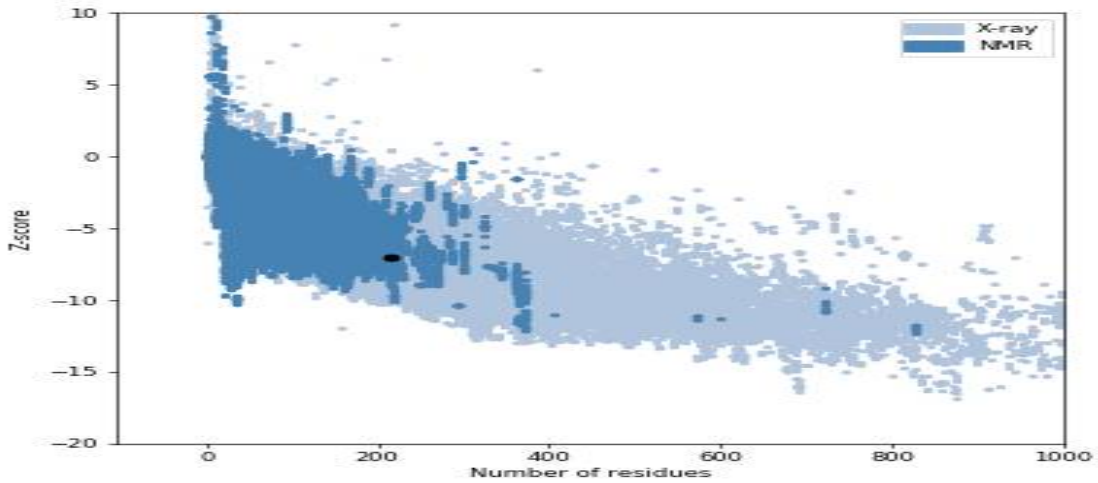

Figure 4: Assessment of the RhoJ protein Overall model quality

Figure 4 illustrates the ProSA analysis of the RhoJ protein, including its Z-score, which serves as an indicator of the model's overall structural quality. The obtained Z-score of -7.07 suggests that the predicted 3D structure of RhoJ closely aligns in quality with experimentally determined crystal structure of proteins in the Protein Data Bank (PDB) that possess a comparable amino acid length.

The overall Z-score of the RhoJ protein, as shown in Figure 4, is -7.07. This value falls within the typical range observed for experimentally resolved protein structure of similar size, determined by X-ray crystallography (light blue) and NMR spectroscopy (dark blue), indicating that RhoJ model is of acceptable overall quality. In addition, the ProSA energy profile provides insights into the local structural quality based on knowledge-based energy calculations. Figure 5 presents the energy distribution across the RhoJ sequence, plotted using two sliding window sizes (10 and 40 amino acids), highlighting region specific stability within the modeled structure.

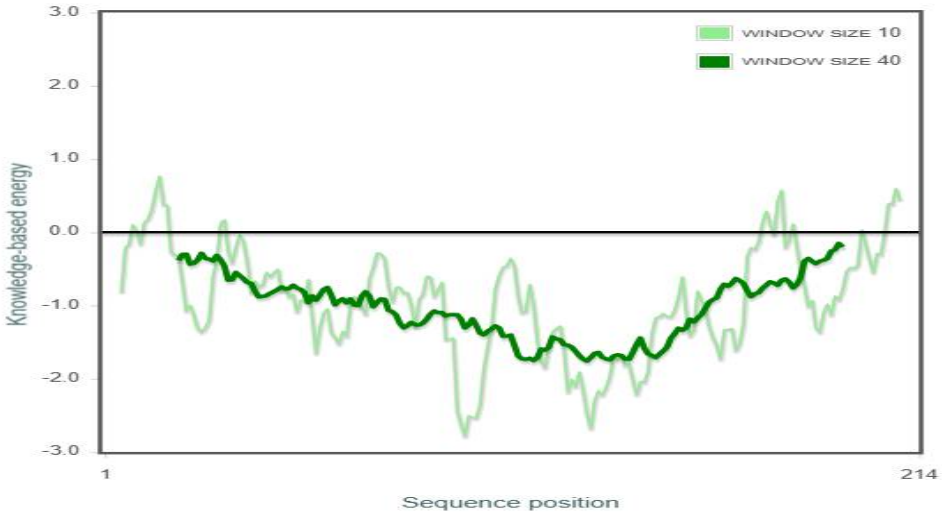

Figure 5. RhoJ protein - Local model quality

Figure 5 shows the RhoJ protein model's local quality score with its respective knowledge-based energy, separately for each of the 19 amino acids. The score is calculated using a sliding window of both 10 (light green) and 40 (dark green) residues. For the most part, the score is situated beneath the baseline, indicating a high likelihood of having favorable local structural quality at any given position in the structure of the protein model.

e) Local Structural motifs analysis

The 3D structure of the RhoJ protein comprises of 7α helices and 6 β-sheets (Figure 6 and Table 2).

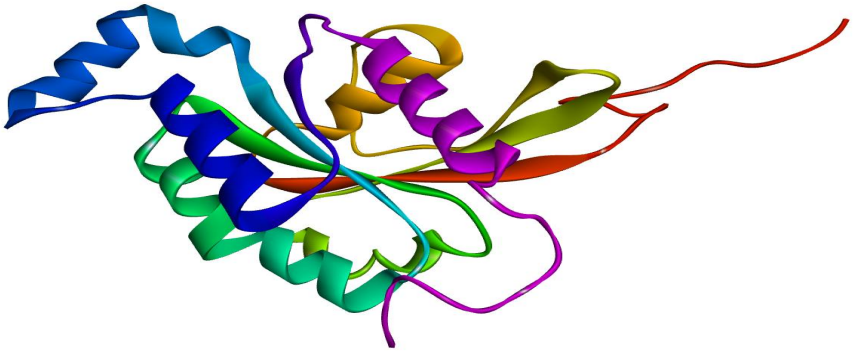

Figure 6: Three – dimensional structure of RhoJ protein

Figure 6 illustrates the ribbon model of the RhoJ protein, the three-dimensional configuration reveals that RhoJ comprises 7 α helices, 6 β-sheets.

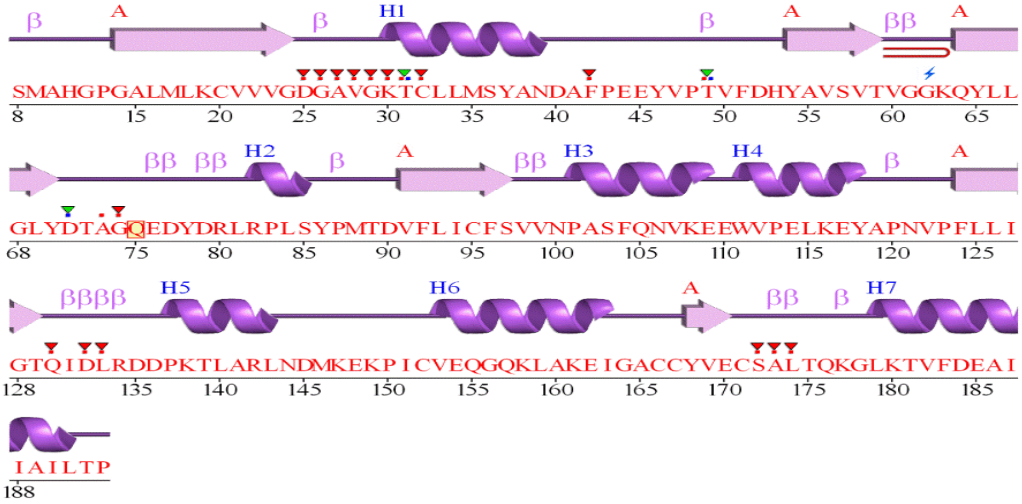

Figure 7: Analysis of the secondary structure of RhoJ protein

Figure 7 presents a schematic representation of the RhoJ protein's secondary structure, generated using the PDBsum server [38, 39]. This diagram highlights the structural elements of RhoJ in conjunction with its amino acid residue composition. The wireframe visualization depicts secondary structure motifs, with α-helices shown in violet, β-sheets indicated by pink arrows.

Table 2: Analysis of secondary structure of the RhoJ protein

S. NO.	Type of Secondary Structure	Amino acids From to To
1	α - helices	ASP 29 to SER 40 ASP 81 to ARG 86 PHE 100 to ASN 110 VAL 111 to LEU 119 ASP 136 to LEU 144 GLU 152 to ALA164 LEU178 to LEU 192
2	β - sheets	ASN 16 to VAL 25 VAL 54 to VAL 60 THR 63 to LEU 70 PRO 91 to ILE 98 MET 123 to VAL 129 ILE 167 to CYS 171

Table 2 lists the secondary structure of RhoJ protein which consists of 7 α – helices and 6 β – sheets.

The putative active site identification

In silico approaches, including CASTp and SiteMap, have been employed to predict potential binding site regions within the RhoJ protein. The CASTp server identifies and evaluates binding pockets by analyzing both the molecular surface (Connolly's surface) and the solvent-accessible surface (Richard's surface) models.

Table 3: The putative active site residues of RhoJ protein

S.NO.	Active site prediction server / tool	Site number	Amino acids	Volume (Å)
1	CASTp	I	20,22,69,92,93, 94,116,119,120, 123,124,125, 126,127,128, 167,168,169, 170,193,194, 195,196,197, 198,201,202, 203,204,205, 206,207,208, 209,210,211, 212	521.144
2	SiteMap	I	20,22,93,94, 120,124,125, 126,127,128, 168,169,170, 193,194,195, 196,197,198, 199,201,202, 203,204,205, 206,207,208, 209,210,211, 212	633.178

The binding cavity data identified by different computational tools are summarized in the table. CASTp identified one binding site, which is comparatively equal in volume identified by SiteMap.

Virtual screening and molecular Docking

This study employs a structure-based virtual screening (SBVS) approach to identify novel small-molecule targeting the RhoJ protein. A receptor grid was defined at the active site of RhoJ with dimensions of 33Å × 10Å × 42Å to facilitate docking simulations. Ligand preparation was conducted using the LigPrep module of the Schrodinger suite, which generated energetically favorable conformers for each input molecule. Multiple ionization states were computed, and tautomeric forms were predicted using the Epik program within LigPrep, which applies Hammett and Taft equations to produce up to eight tautomeric variants per ligand by default. Structural anomalies-such as geometric violations in fused ring systems or chirality

mismatches in natural products – were automatically corrected to ensure the resulting ligands possessed appropriate stereochemistry, low-energy ring conformations, and acceptable ionization states. A total of 30,000 compounds from the comprehensive marine natural products database (CMNPD) [40]-[42] were processed, resulting 45,801 distinct ligand structures. These ligands were subjected to a multi-tier virtual screening workflow using Glide (Glide, version, Schrödinger, LLC, New York, NY, 2023) comprising High Throughput Virtual Screening (HTVS), Standard Precision (SP), and Extra Precision (XP) docking protocols. At each stage, approximately 10% of the input ligands with optimal binding poses were retained, following the program's default filtering strategy.

The final output included 5 top-ranked docked ligand-RhoJ complexes. A representative subset of five ligands, prioritized by Glide docking scores, is presented in Figure 8 and Table 4. Comparable SBVS [43] [44] methodologies have been employed in prior studies for the identification of novel lead compounds against emerging drug targets.

Detailed analysis of the docking results revealed favorable ligand-protein interactions, indicating high binding affinity. Hydrogen bonding interactions within the complexes were visualized using Accelrys Discovery Studio Visualizer [45], with all hydrogen bond distances falling within a significant range of 1.58 to 2.76Å (Table 4). The corresponding 3D-2D interactions of selected ligand (D1-D5) - RhoJ complexes are illustrated in Figure 8.

Table 4: Ligands (D1 to D5) interaction with RhoJ protein

Serial Number	Ligand (D)	Glide Score	Glide Energy (kcal/mol)	Hydrogen Bond	H –Bond Distance (Å)
D1	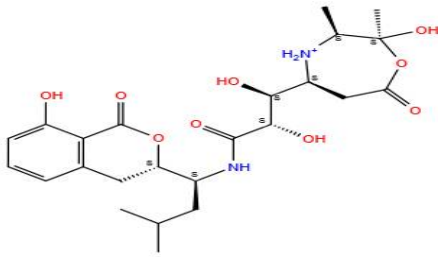	-9.089	-58.507	D1 - LYS 198 D1- ARG 203(1) D1–ARG 203 (2) D1- ASP 094(1) D1- ASP 094(2) D1- ASP 094 (3) D1- ASP094 (4) D1 - ILE 194	2.42 2.53 2.19 2.27 2.27 1.60 1.58 2.08
D2	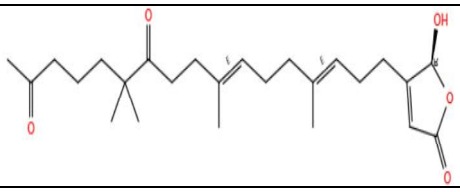	-8.080	-43.996	D2-SER 212 D2-TYR128(1) D2-TYR 128(2) D2-SER 209 D2-PRO124	1.82 1.92 1.92 2.16 1.82
D3	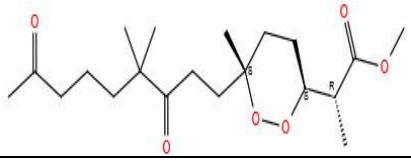	-8.014	-43.307	D3–GLY 207 D3- LYS198 D3-TYR 128	2.76 2.24 2.31
D4	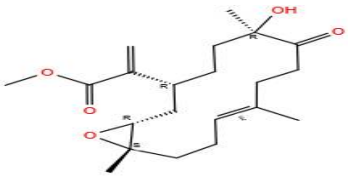	-7.874	-38.144	D4 - CYR 204 D4 - ILE 194	1.86 2.56
D5	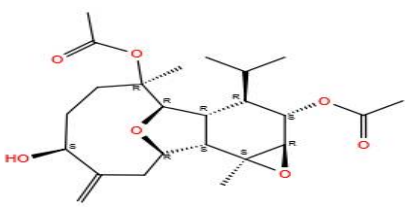	-7.260	-40.628	D5 - SER 204 D5 - ASP 094	2.24 1.84

D1 –Rho J protein interactions

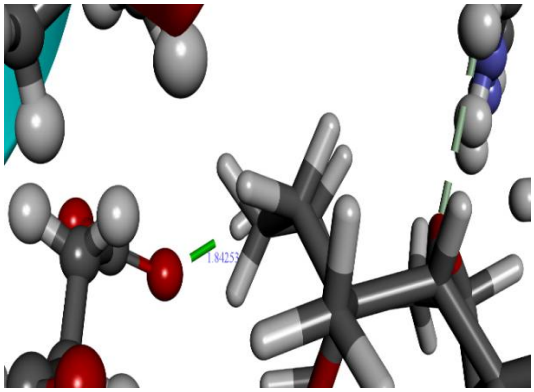

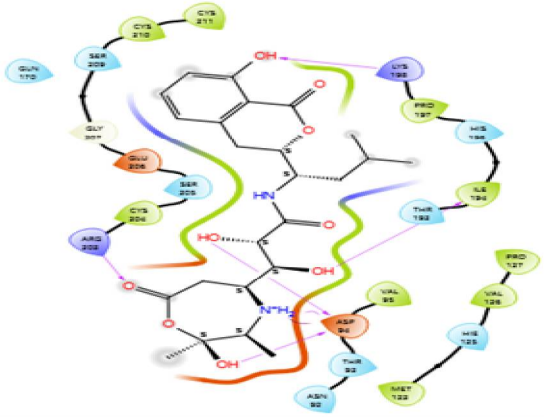

D2 – RhoJ protein interactions

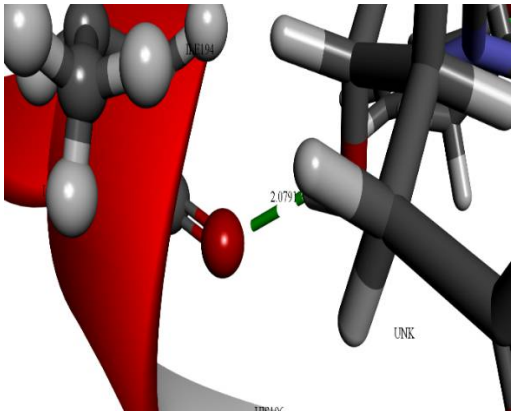

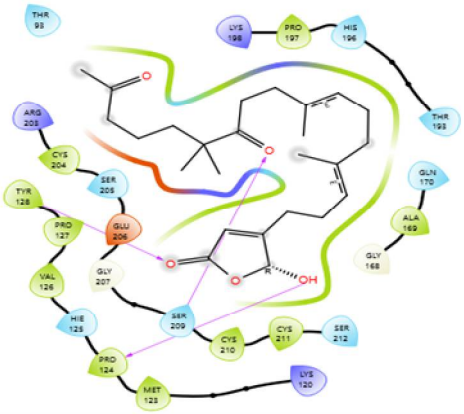

D3 – RhoJ protein interactions

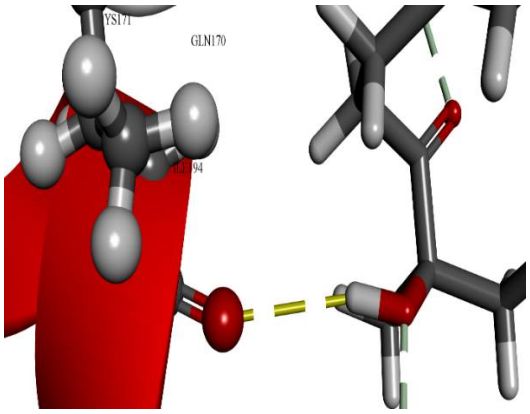

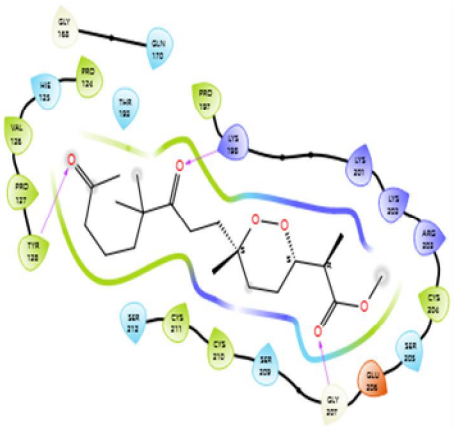

D4 – RhoJ protein interactions

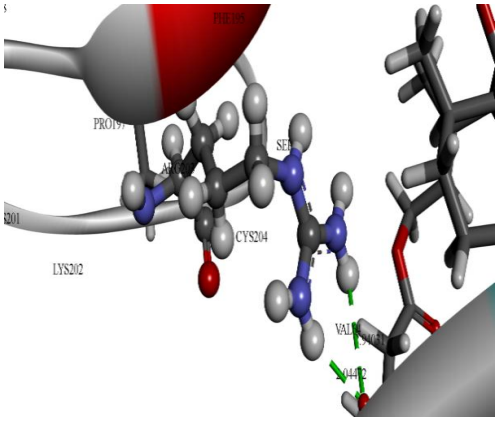

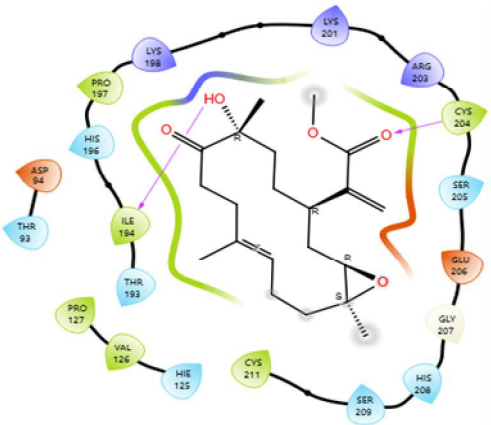

D5 – RhoJ protein interactions

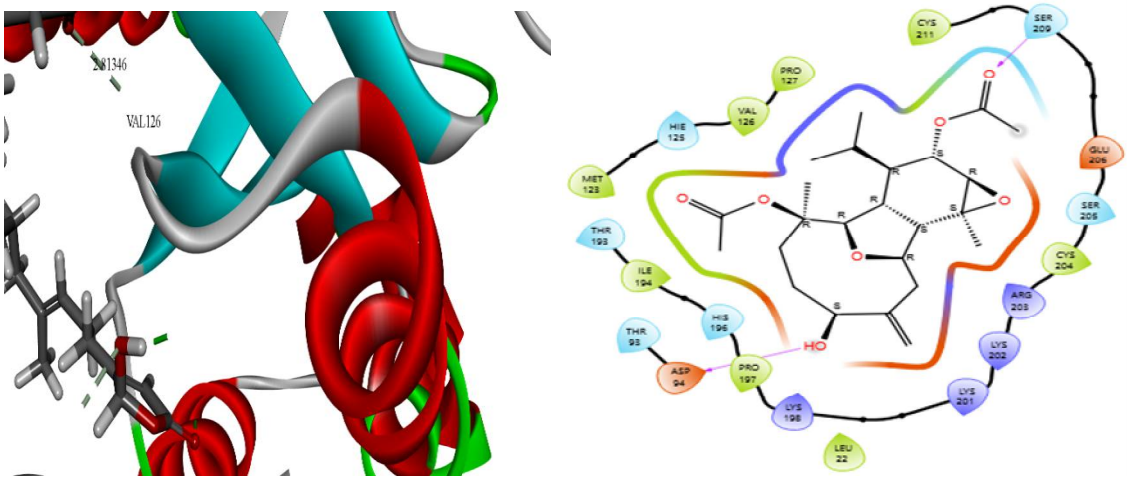

Figure 8: RhoJ protein interaction with new leads

ADME (Absorption, Distribution, Metabolism, and Excretion)

Physicochemical properties

Preclinical evaluation represents a critical phase in the drug discovery pipeline. In this study, ADME profiling was conducted newly identified ligands and utilizing the QikProp [46] module within the Schrodinger suite (Table 5). Key physiochemical parameters, including molecular weight (≤500Da), along with hydrogen bond order (DHB) and acceptor (AHB) counts, were found to fall within acceptable ranges (DHB≤5; AHB≤13), as detailed in Table 5.

Table 5: Calculated ADME properties of ligands (D1 to D5)

Ligand Number	Physicochemical Properties				Pharmacokinetic Properties							Drug Likeness Properties		
	Mol MW	Donor HB	Accept HB	QP logS	HOA%	QP PCaco	QP log Khsa	QP log Pw	QP log BB	CNS	QP log HERG	Rule Of Five	Rule Of Three	QP log Po/w
D1	494.544	4	12.9	-2.607	86.338	75.302	-0.619	21.475	-2.433	-2	-4.774	2	1	0.171
D2	418.572	1	8.7	-5.514	84.941	157.065	0.297	10.016	-2.477	-2	-5.467	1	0	3.784
D3	370.485	0	8.45	-3.103	88.138	418.584	-0.392	8.465	-1.445	-2	-4.299	0	0	2.437
D4	356.481	1	6.75	-4.548	100	1595.495	0.407	9.402	-0.339	0	-3.624	0	0	3.357
D5	436.546	1	9.4	-3.577	100	1121.173	0.075	11.841	-0.487	-1	-3.117	0	0	2.667

Pharmacokinetic properties

Human oral absorption (HOA) is a key pharmacokinetic parameter in the early stages of drug development. All candidate's ligands evaluated in this study demonstrated favorable HOA values, ranging from 86.338 % to 100 %, indicative of good oral bioavailability. All screened ligands fall within acceptable limits for oral absorption (Table 6).

Aqueous solubility, which plays a vital role in determining a compound's absorption and systemic distribution, was assessed using QPlogs descriptor. The solubility values for the ligands ranged between -2.607 to -5.514 which is considered acceptable. The QPPCaco descriptor, which estimates permeability across the intestinal epithelium, revealed values between 75.302 and 1595.495, indicating that the ligands possess suitable permeability to cross the gut – blood barrier. Protein binding, especially to serum albumin, can significantly affect the pharmacokinetic behavior of drugs. Therefore, QPlogKhsa values were calculated to assess human serum albumin binding affinity. The ligands exhibited values ranging from - 0.619 to 0.407, falling within acceptable pharmacological limits [47-49] (Table 6).

Table 6: Permissible Values of ADME

S. No.	Descriptor	ADME Property	Permissible Ranges or Recommended Value
1	**CNS**	Predicted central nervous system activity on -2 to +2 scale	–2 (inactive) to +2 (active)
2	**mol_MW**	Molecular weight of the molecule	130 to 725
3	**DHB**	Estimated number of hydrogen bonds donated by solute in aqueous solution	0 to 6
4	**AHB**	Estimated number of hydrogen bonds accepted by solute in aqueous solution	2 to 20
5	**QPPcaco**	Predicted Caco-2 cell permeability (nm/sec)	<25 = poor, >500 = great
6	**QP logPw**	Predicted water/gas partition coefficient	4.0 – 45.0
7	**QP logPo/w**	Predicted octanol/water partition coefficient	–2.0 – 6.5
8	**QP logS**	Predicted aqueous solubility, log S (mol/dm^3)	–6.5 – 0.5
9	**QP logKhsa**	Predicted binding to human serum albumin	–1.5 – 1.5
10	**QP logHERG**	Predicted IC_{50} for blockage of HERG K^+ channels	Below +5.0
11	**QP logBB**	Predicted blood/brain partition coefficient	–3.0 – 1.2
12	**% Human Oral Absorption**	Predicted human oral absorption on 0 to 100% scale	>80% = high; <25% = poor
13	**Rule Of Five**	Number of violations of Lipinski's Rule of Five	Maximum is 4
14	**Rule Of Three**	Number of violations of Jorgensen's Rule of Three	Maximum is 3
15	**Synthetic Feasibility**	Predicted synthetic feasibility on scale of 1 to 10	0 = high feasibility, 10 = least feasible
16	**Lipophilicity**	Predicted lipophilic nature (pIC50 – LogP)	min -6; max +3

Given the potential adverse effects of inappropriate blood-brain barrier (BBB) permeability on the central nervous system (CNS), QPlogBB values were also analyzed. All ligands showed acceptable values within the range of -2.477 to -0.339, suggesting limited CNS penetration. Moreover, CNS activity scores were negative for all compounds, indicating a low risk of neurotoxicity and implying CNS safety.
Finally, inhibition of the human ether-a-go-go-related gene (hERG) potassium channel is a known concern in cardiac safety due to its association with prolonged QT intervals and potential arrhythmias. The predicted pIC50 values for hERG K+ channel inhibition ranged from -5.467 to -3.117 for all ligands, suggesting a low risk of cardiotoxicity.

Table 7: Toxicity Profile: Predicted Toxic profile of ligands (D1 to D5) using Pro Tox 3.0 server

Ligand	CYP1A2	CYPC19	CYP2C9	CYP2D6	CYP3A4
D1	Negative	Negative	Negative	Negative	Negative
D2	Negative	Negative	Negative	Negative	Negative
D3	Negative	Negative	Negative	Negative	Negative
D4	Negative	Negative	Negative	Negative	Negative
D5	Negative	Negative	Negative	Negative	Negative

Table 7 summarizes the calculated toxicological impact of ligands D1 to D5 on the cytochrome P450 enzyme system. It indicates whether each ligand, along with standard cancer drugs, functions as a non-inhibitor of the P450 enzymatic activity [50].

CONCLUSION

The present in silico investigation provides a comprehensive evaluation of RhoJ, a critical regulator of angiogenesis and cytoskeletal dynamics implicated in various cancers. Using homology modeling, a reliable 3D structural model of RhoJ was developed and validated through robust tools such as Ramachandran plot, ProSA, and Verify3D. Active site prediction using CASTp and SiteMap enabled precise localization of potential binding pockets. Structure-based virtual screening of marine natural product libraries led to the identification of five top-ranking ligands (D1–D5) with strong binding affinities to key residues like ARG203, ILE194, TYR128, ASP94, and LYS198. These ligand–protein complexes demonstrated high docking scores and favorable hydrogen bonding interactions, confirming their stability and specificity. The ADMET analysis revealed all ligands had acceptable physicochemical and pharmacokinetic profiles, including high human oral absorption, ideal molecular weight, solubility, and permeability. None of the compounds inhibited major cytochrome P450 enzymes, minimizing potential toxicity or drug–drug interactions. Importantly, all ligands demonstrated low hERG inhibition and CNS

activity, suggesting excellent safety profiles. These findings suggest that the selected ligands are promising candidates for further development as targeted inhibitors of RhoJ, with potential therapeutic applications in cancer treatment. Future *in vitro* and *in vivo* validations will be necessary to confirm their efficacy and pharmacological viability.

REFERENCES

1. Kaur, S., Leszczynska, K., Abraham, S., Scarcia, M., Hiltbrunner, S., et al. (2011). RhoJ/TCL regulates endothelial motility and tube formation and modulates actomyosin contractility and focal adhesion numbers. Arteriosclerosis, Thrombosis, and Vascular Biology, 31(3), 657–664.
2. Ho, H., et al. (2013). RhoJ modulates melanoma invasion by altering actin cytoskeletal dynamics. Pigment Cell & Melanoma Research. doi: 10.1111/pcmr.12058. Epub 2013 Jan 7.
3. Wang, M., Zhang, C., Zheng, Q., Ma, Z., Qi, M., Di, G., Ling, S., Xu, H., Qi, B., Yao, C., Xia, H., & Jiang, X. (2022). RhoJ facilitates angiogenesis in glioblastoma via JNK/VEGFR2 mediated activation of PAK and ERK signaling pathways. International Journal of Biological Sciences, 18(3), 942–955. doi:10.7150/ijbs.65653
4. Gu, F., et al. (2013). Vascular RhoJ Is an Effective and Selective Target for Tumor Angiogenesis and Vascular Disruption. Cancer Cell. doi: 10.1016/j.ccr.2013.12.010.
5. Cao, J., Xie, X., Han, L., Rhee, H. W., et al. (2020). MKL1 mediates TGF-β induced RhoJ transcription to promote breast cancer cell migration and invasion. Frontiers in Cell and Developmental Biology, 8, 832.
6. Ruiz, R., Jahid, S., Harris, M., Marzese, D. M., Espitia, F., et al. (2017). The RhoJ-BAD signaling network: An Achilles' heel for BRAF mutant melanomas. PLoS Genetics, 13(5), e1006913.
7. Shi, T. T., & Xiao, H. T. (2016). The role of RhoJ in endothelial cell biology and tumor pathology. BioMed Research International, 2016, 6386412.
8. Maud Debaugnies, et al. (2024). The discovery of a protein controlling resistance to chemotherapy [RhoJ in EMT-related chemoresistance]. ecancer News.
9. Kim, C., Yang, H., Fukushima, Y., Saw, P. E., Lee, J., Park, J. S., et al. (2014). Vascular RhoJ is an effective and selective target for tumor angiogenesis and vascular disruption. Cancer Cell, 25(1), 102–117.
10. Debaugnies, M., Rodríguez-Acebes, S., Blondeau, J., Parent, M.-A., Zocco, M., Song, Y., et al. (2023). RHOJ controls EMT-associated resistance to chemotherapy. Nature. **616**, 168–175 (2023). https://doi.org/10.1038/s41586-023-05838-7
11. Ma, Z., Sun, Q., Zhang, C., Zheng, Q., Liu, Y., Xu, H., He, Y., Yao, C., Chen, J., & Xia, H. (2023). RHOJ Induces Epithelial-to-Mesenchymal Transition by IL-6/STAT3 to Promote Invasion and Metastasis in Gastric Cancer. International Journal of Biological Sciences, 19(14), 4411–4426. doi:10.7150/ijbs.81972
12. Lu, X. J., Lai, H. F., Wu, S. C., Chen, C. L., & Chiu, Y. L. (2023). Elucidating the associated biological function and clinical significance of RHOJ expression in urothelial carcinoma. International Journal of Molecular Sciences, 24(18), 14081.
13. Sundararaman, A., Fukushima, Y., Norman, J. C., et al. (2020). RhoJ regulates α5β1 integrin trafficking to control fibronectin remodeling during angiogenesis. Current Biology, 30(11), 2146–2155.
14. Liu, S., Ren, J., & Zhang, L. (2023).Ras homolog family member J (RHOJ): a key regulator of chemoresistance associated with epithelial-mesenchymal transition. Signal Transduction and Targeted Therapy, 8, Article 62.
15. The UniProt Consortium. (2023). UniProt: the Universal Protein Knowledgebase in 2023. Nucleic Acids Research, 51(D1), D523–D531. https://doi.org/10.1093/nar/gkac1052
16. Drozdetskiy, A., Cole, C., Procter, J., & Barton, G. J. (2015). JPred4: a protein secondary structure prediction server. Nucleic Acids Research, 43(W1), W389–W394. https://doi.org/10.1093/nar/gkv332
17. Kelley, L. A., et al. (2015). The Phyre2 web portal for protein modeling. Nature Protocols, 10(6), 845–858. https://doi.org/10.1038/nprot.2015.053
18. Thompson, J. D., et al. (1994). CLUSTAL W: improving the sensitivity of progressive multiple sequence alignment. Nucleic Acids Res, 22(22), 4673–4680.
19. Webb, B., & Sali, A. (2016). Comparative protein structure modeling using MODELLER. Current Protocols in Bioinformatics, 54(1), 5.6.1–5.6.37. https://doi.org/10.1002/cpbi.3
20. Friesner, R. A., Banks, J. L., Murphy, R. B., Halgren, T. A., et al. (2004). Glide: A new approach for rapid, accurate docking and scoring. 1. Method and assessment of docking accuracy.Journal of Medicinal Chemistry, 47(7), 1739–1749. https://doi.org/10.1021/jm0306430
21. Laskowski, R. A., MacArthur, M. W., Moss, D. S., & Thornton, J. M. (1993). PROCHECK: A program to check the stereochemical quality of protein structures. Journal of Applied Crystallography, 26(2), 283–291. https://doi.org/10.1107/S0021889892009944
22. Wiederstein M & Sippl MJ (2007) ProSA-web: interactive web service for the recognition of errors in three-dimensional structures of proteins. Nucleic Acids Res 35, W407–W410
23. Lüthy, R., Bowie, J. U., & Eisenberg, D. (1992). Assessment of protein models with three-dimensional profiles. Nature, 356(6364), 83–85. https://doi.org/10.1038/356083a0
24. Tian, W., et al. (2018). CASTp 3.0: computed atlas of surface topography of proteins. Nucleic Acids Res, 46(W1), W363–W367. https://doi.org/10.1093/nar/gky473
25. Halgren, T. A. (2009). Identifying and characterizing binding sites and assessing drug ability. Journal of Chemical Information and Modeling, 49(2), 377–389. https://doi.org/10.1021/ci800324m

26. Sastry, G. M., Adzhigirey, M., Day, T., Annabhimoju, R., & Sherman, W. (2013). Protein and ligand preparation: Parameters, protocols, and influence on virtual screening enrichments. Journal of Computer-Aided Molecular Design, 27(3), 221–234.
27. R Dumpati, V Ramatenki, R Vadija, S Vellanki, U Vuruputuri. (2018). Structural insights into suppressor of cytokine signaling 1 protein-identification of new leads for type 2 diabetes mellitus, Journal of Molecular Recognition 31 (7), e2706
28. R Dumpati, R Dulapalli, B Kondagari, V Ramatenki, S Vellanki, R Vadija. (2016). Suppressor of cytokine signalling-3 as a drug target for type 2 diabetes mellitus: a structure-guided approach, Chemistry Select 1 (10), 2502-2514
29. Muddagoni et al. (2021): Homology modeling validated with ProSA and Verify3D; binding-site identification via SiteMap; virtual screening using Schrödinger suite (LigPrep → Glide docking → QikProp ADME profiling)
30. Banerjee, P., et al. (2018). ProTox-II: prediction of toxicity of chemicals. Nucleic Acids Res, 46(W1), W257–W263. https://doi.org/10.1093/nar/gky318
31. Drwal, M. N., Banerjee, P., Dunkel, M., Wettig, M. R., & Preissner, R. (2014). ProTox: a web server for the in silico prediction of rodent oral toxicity. Nucleic Acids Research, 42(W1), W53–W58.
32. Altschul, S. F., Gish, W., Miller, W., Myers, E. W., & Lipman, D. J. (1990). Basic local alignment search tool. Journal of Molecular Biology, 215(3), 403–410. https://doi.org/10.1016/S0022-2836(05)80360-2
33. Burley, S. K., Berman, H. M., Bhikadiya, C., Bi, C., Chen, L., et al. (2021). RCSB Protein Data Bank: Powerful new tools for exploring 3D structures of biological macromolecules for basic and applied research and education. Nucleic Acids Research, 49(D1), D437–D451. https://doi.org/10.1093/nar/gkaa1038
34. Webb, B., & Sali, A. (2016). Comparative protein structure modeling using MODELLER. Current Protocols in Bioinformatics, 54(1), 5.6.1–5.6.37. https://doi.org/10.1002/cpbi.3
35. Laskowski, R. A., MacArthur, M. W., Moss, D. S., & Thornton, J. M. (1993). PROCHECK: A program to check the stereochemical quality of protein structures. Journal of Applied Crystallography, 26(2), 283–291. https://doi.org/10.1107/S0021889892009944
36. Bhargavi, M., & Bhargavi, S. G. (2025). Computational approach for HDAC1 predicting protein–ligand interactions for cancer through homology modelling, virtual screening and molecular docking. Shanlax Publications–Computational Technology & Biology. https://www.shanlaxpublications.com/p/ctbtls/ch002.pdf
37. Laskowski, R. A. (2001). PDBsum: summaries and analyses of PDB structures. Nucleic Acids Research, 29(1), 221–222. https://doi.org/10.1093/nar/29.1.221
38. Laskowski, R. A., Jabłońska, J., Pravda, L., Vařeková, R. S., & Thornton, J. M. (2018). PDBsum: Structural summaries of PDB entries. Protein Science, 27(1), 129–134. https://doi.org/10.1002/pro.3289
39. Laskowski, R. A., & Thornton, J. M. (2022). PDBsum extras: SARS-CoV-2 and AlphaFold models. Protein Science, 31(1), 184–186.
40. Lyu C, Chen T, Qiang B, Liu N, Wang H, Zhang L, Liu Z. (2021). CMNPD: a comprehensive marine natural products database towards facilitating drug discovery from the ocean. Nucleic Acids Res.8;49(D1):D509-D515. doi: 10.1093/nar/gkaa763. PMID: 32986829; PMCID: PMC7779072.
41. Afendi, F. M., Okada, T., Yamazaki, M., Hirai-Morita, A., Nakamura, Y., Nakamura, K., ... & Saito, K. (2020). CMNPD: A comprehensive marine natural products database towards facilitating drug discovery from the ocean. Nucleic Acids Research, 48(D1), D509–D516. https://doi.org/10.1093/nar/gkz890
42. Bhat, B. A., Algaissi, A., Khamjan, N. A., Dar, T. U. H., & Qasir, N. (2024). Exploration of CMNPD against Dengue viral NS1 protein using high-throughput computational studies. Journal of Biomolecular Structure and Dynamics. https://doi.org/10.1080/07391102.2023.2297006
43. Jin, F., Singh, P., Chen, H., & Deng, Y. (2025). AI-guided discovery of small molecules targeting eIF4F complex to inhibit oncogenic mRNA translation in castration-resistant prostate cancer. Cancer Research, 85(8_Supplement_1), 7437.
44. Rocca, R., Alcaro, S., & Artese, A. (2024). Structure-based virtual screening and molecular dynamics simulations of FDA-approved drugs targeting MALAT1. *Med Chem Res* **33**, 2095–2100 (2024). https://doi.org/10.1007/s00044-024-03336-7
45. BIOVIA, Dassault Systèmes. (2020). Discovery Studio Modeling Environment, Release 2020. San Diego, CA: Dassault Systèmes.
46. Chikhale, H. U., & Rishipathak, D. D. (2025). In silico prediction, molecular docking study for identification of novel nitrogen-substituted benzoxazole derivative for their potential biological activity. *Chemistry Africa* **8**, 909–921 (2025). https://doi.org/10.1007/s42250-025-01208-0
47. Lipinski, C. A., Lombardo, F., Dominy, B. W., & Feeney, P. J. (2001). Experimental and computational approaches to estimate solubility and permeability in drug discovery and development settings. Advanced Drug Delivery Reviews, 46(1–3), 3–26. https://doi.org/10.1016/S0169-409X(00)00129-0
48. Ibrahim, Z. Y., Abdulfatai, U., Ejeh, S., Ajala, A., & Adawara, S. N. (2024). QSAR and ADMET screening to assess antimalarial potential of Amodiaquine derivatives. The Microbe. https://doi.org/10.1016/j.microb.2024.100208
49. Mohamed, S. S., Bensaber, S. M., Meiqal, N. H. (2025). Design and in-silico evaluation of pyridine-4-carbohydrazide derivatives. Journal of Surgical Case Reports. https://doi.org/10.31579/2690-1897/235

50. Aryal B, Raut BK, Bhattarai S, Bhandari S, Tandan P, Gyawali K, Sharma K, Ranabhat D, Thapa R, Aryal D, Ojha A, Devkota HP, Parajuli N. (2022). Potential Therapeutic Applications of Plant-Derived Alkaloids against Inflammatory and Neurodegenerative Diseases. Evid Based Complement Alternat Med. 2022 Mar 9;7299778. doi: 10.1155/2022/7299778. PMID: 35310033; PMCID: PMC8926539.